SUPPLEMENTARY FILE

To cite this article: Ramiaramanana, F. N., Munyi, Jm.M, Archambeau, P., Teller, J. (2025). A comparative assessment of flood mapping methods for urban risk management in data-poor environments. Nat Hazards (2025). https://doi.org/10.1007/s11069-025-07590-9.

PART 1. DETAILS OF THE DATA USED

1. Technical specifications

- The spatial resolutions indicated refer to the nominal pixel sizes of each dataset. Minor variations may occur due to projection transformations and data processing. For instance, Sentinel-1 data typically have pixel dimensions of approximately 10.06 × 10.44 meters, while the Copernicus Digital Elevation Model (DEM) presents values close to 30.00 × 30.01 meters.
- The flood event that occurred between 18 and 29 January 2022 in Antananarivo was selected for its exceptional scale. This was triggered by extreme precipitation linked to an intertropical convergence zone and the passage of a cyclone (Rakotoarimanana and Rakotovao 2022). The satellite imagery used corresponds to data available for this period. For the FastFlood Simulation (FFS) model, 24 January 2022 was chosen specifically because of a peak rainfall intensity of 31 mm/h recorded at 7:00 a.m. (Anosizato station). Although rainfall measurements for that day are limited and spatially isolated, the intensity was considered representative of a significant rainfall episode, justifying its use in simulating a critical flood scenario.

2. Parameter-specific notes

Table S1. Dataset-specific notes

Parameter	Source and description
Digital Elevation Model (DEM)	A Copernicus DEM at 30 m resolution, with a vertical accuracy of < 4 m at the 90% confidence level (Fahrland et al. 2022)
Surface Roughness	Derived from Copernicus WorldCover; Manning values assigned using FastFlood's land cover lookup table (Van den Bout 2024)
Infiltration Rates	Based on SoilGrids (ISRIC); downloaded via FastFlood for a depth of 5–15 cm depth, assigned via a lookup table by soil type (Van den Bout 2024)

PART 2. TECHNICAL SPECIFICATIONS OF THE FLOOD MAPPING APPROACHES

1. Summary of technical details of flood mapping methods

Table S2. Overview of methods and processing characteristics

Component	Pleiades imagery	Sentinel-1 imagery	FFS	MCA
Data type / model	Very high-resolution satellite imagery (optical)	Synthetic Aperture Radar (SAR)—IW mode, VV/VH polarizations	Simplified hydrological simulation model	GIS-based composite index model using geographic and climatic indicators
Data accessibility	Commercial	Free and open access	Open access	Open access
Spatial resolution	2 m × 2 m	10 m × 10 m	30 × 30 m (DEM resolution)	Variable
Input data	Pleiades (28/01/2022)	Sentinel-1 (27/01/2022)	DEM, rainfall, roughness, infiltration	DEM, land use, NDVI, lithology, precipitation, slope, TWI, SPI, distance to rivers

Processing / Analysis	- OBIA approach - Mean shift segmentation (8-neighbor) - Zonal stats (mean, std. dev.) - SVM classification (LibSVM via OTB) (Ramdani 2023; Recanatesi et al. 2025) - 1,400 training samples - Manual post-classification using building vectors	- Preprocessing: radiometric calibration, speckle filtering, terrain correction (Denis 2019; McVittie 2019a) - Conversion of backscatter values to dB $\sigma_0^{dB} = 10 * log_{10}(\sigma_0)$ (Laur et al. 2002) - Manual thresholding (Selmi 2021)	- DEM correction via Fast Sweeping Method (FSM) - Steady-state flow simulation - Manning-based water depth calculation - Compensation scheme based on slope and distance to outlet - Diffusive wave solver - Calibration with four parameter sets (*) - Sensitivity analysis	- Normalization and quantile classification - Equal weighting - Composite flood susceptibility index
Output format	Flood extent Vector > Raster (2 m)	Flood extent Raster (10 m)	Modeled flood-prone areas with depth classification Raster (30 m)	Flood susceptibility map with five risk levels Raster (30 m)
Software	QGIS, Orfeo Toolbox (OTB)	SNAP (ESA)	FastFlood App (online); QGIS for post processing	QGIS

(*) Simulations used in FFS:

- Sim 1: DEM, rainfall, homogeneous Manning (0.06), infiltration
- Sim 2: DEM, rainfall, homogeneous Manning (0.06)
- Sim 3: DEM, rainfall, heterogeneous Manning
- Sim 4: DEM, rainfall, heterogeneous Manning, infiltration

2. Indicators used in the flood susceptibility analysis (MCA)

Table S3. Indicators and processing methods

Indicator	Role	Processing method
Altitude (m)	Influences water accumulation in low areas, which are generally more prone to flooding	Extracted from the DEM
Slope (%)	Affects water flow: areas with a low slope retain more water, increasing flood risk	
TWI	Measures a region's ability to accumulate water based on slope and drainage area (Hojati and Mokarram, 2016 ; Nibigira, 2019)	Calculated from the DEM using the following formulas: TWI = ln($\frac{A_S}{\tan \beta}$) (Beven and Kirkby 1979)
SPI	Estimates the river's susceptibility to erosion and characterizes the intensity of surface runoff (Bizzi and Lerner 2015; Khosravi et al. 2019; Nibigira 2019)	SPI = A_s * tan β (Moore et al. 1991) A_S is the specific drainage area (m^2/m), using multidirectional flow direction algorithms (MFD), and β is the local slope angle.
Annual precipitation (mm/year)	Determines the amount of rainfall, directly influencing flood risk	Calculated from monthly averages from 2010 to 2021
Land use (*)	Influences infiltration and runoff: impermeable surfaces increase flood risks	Classified from Landsat images using supervised classification
NDVI (*)	Reflects the density of vegetation, influencing water infiltration and absorption	Calculated from Landsat images: NDVI $=\frac{\mathrm{NIR}-\mathrm{Red}}{\mathrm{NIR}+\mathrm{Red}}$ NIR and Red are spectral bands
Distance from rivers (m)	Helps estimate the vulnerability of areas based on their proximity to rivers	Calculated from hydrographic networks using Euclidean distance analysis, classified into 50 m intervals
Lithology	Influences water infiltration, permeability, and retention capacity (ARTELIA 2020)	Classified based on properties (porosity and permeability) (Andriamamonjisoa and Hubert-Ferrari 2019)

(*) The NDVI and land use indicators used in the MCA were derived from a cloud-free Landsat 8 image acquired on 29/08/2022. Although Sentinel-2 offers higher spatial resolution, Landsat 8 was selected to ensure resolution consistency with other spatial layers (30 m), such as the DEM, altitude, slope, TWI, and SPI. Furthermore, Landsat data were used solely to derive ancillary indicators; they were not used for direct flood detection.

PART 3. CLASSIFICATION ERRORS IN PLEIADES IMAGERY

This figure illustrates some common misclassifications encountered during the processing of the Pleiades imagery.

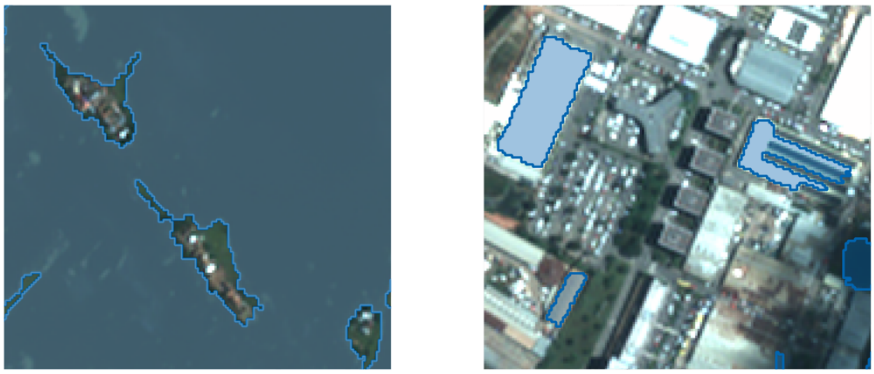

a. Independent zones (isolated buildings) b. Misclassified areas

Fig. S1. Typical classification issues requiring correction

PART 4. RESULTS OF THE FFS MODEL

1. Summary of simulated flood depths across the four scenarios

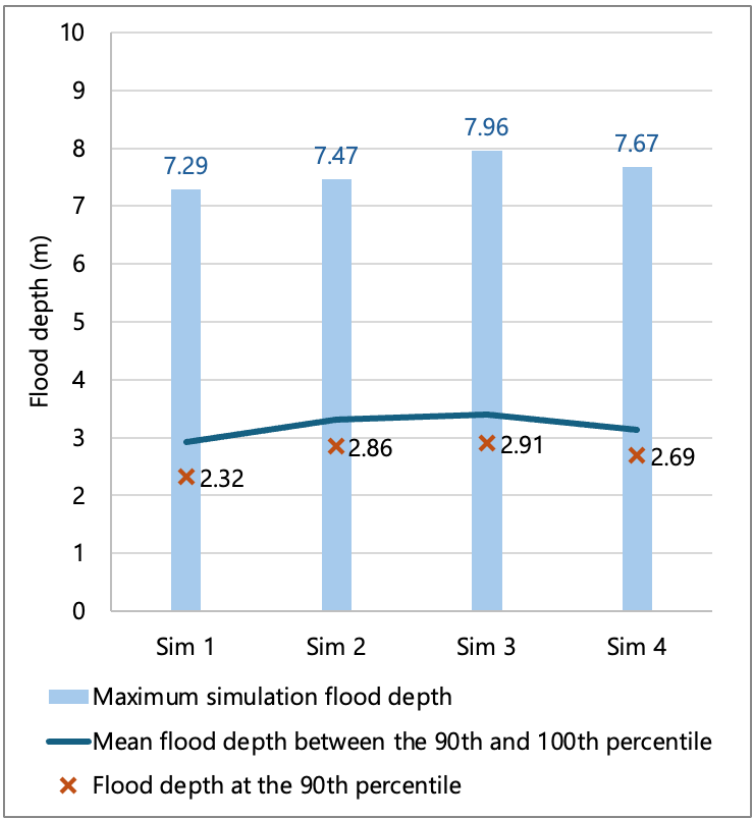

Fig. S2. Changes in simulated flood depths between simulations—10 cm threshol

2. Spatial differences in slope and simulated water depth

The maps in this section illustrate the differences between the raw and hydrologically corrected DEMs.

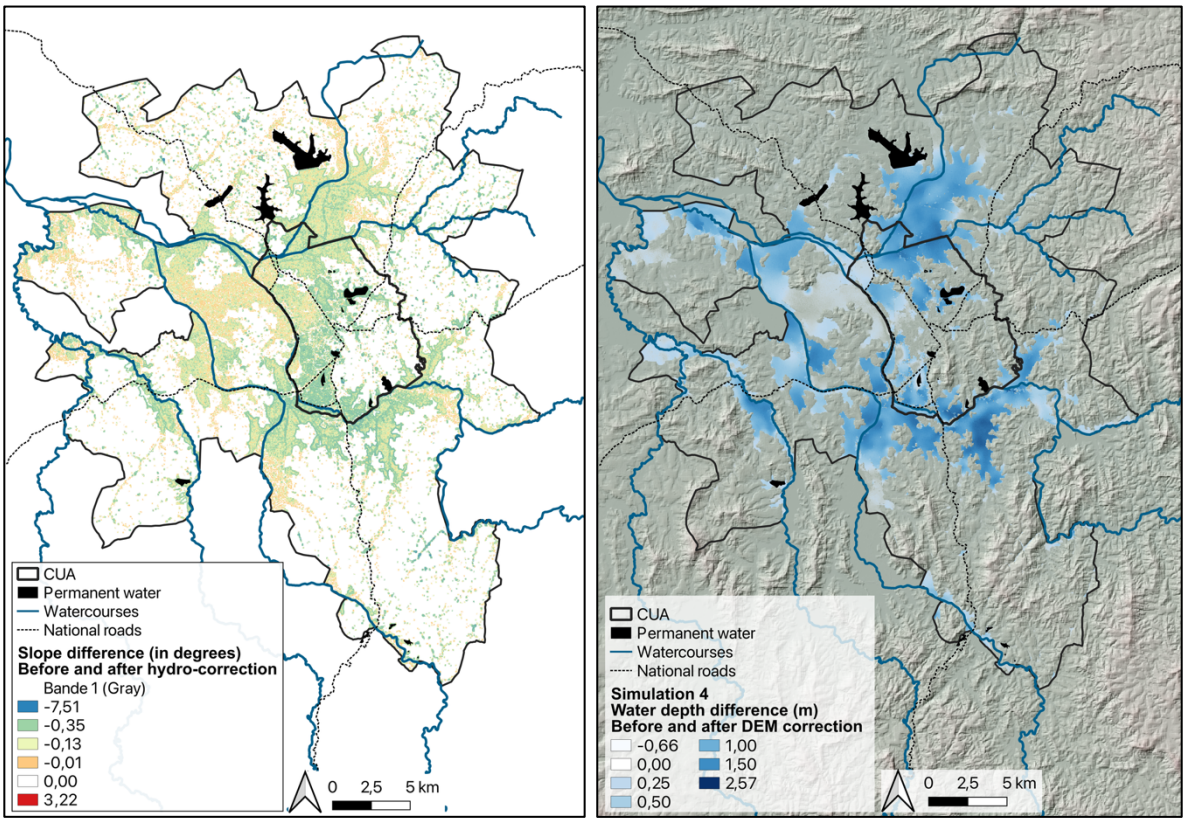

a. Slope difference b. Water depth difference

Fig. S3. Raw and corrected DEM

3. Distribution of simulated water depth by slope class

Table S4. Pixel count distribution across slope and depth classes—comparison between raw and corrected DEM

	Pixel count											
	Depth class (m)											
	Raw DEM						Corrected DEM					
Slope class (°)	**0–0.5**	**0.5–1**	**1–2**	**2–3**	**3–4**	**> 4**	**0–0.5**	**0.5–1**	**1–2**	**2–3**	**3–4**	**> 4**
0–2	114,698 (40.85%)	103,436 (36.84%)	60,403 (21.51%)	2,113 (0.75%)	131 (0.05%)	23 (0.01%)	79,970 (27.11%)	41,305 (14%)	123,781 (41.97%)	49,531 (16.79%)	324 (0.11%)	29 (0.01%)
2–5	152,142 (90.16%)	9,398 (5.57%)	5,978 (3.54%)	954 (0.57%)	250 (0.15%)	29 (0.02%)	142,870 (89.95%)	6,707 (4.22%)	7,423 (4.67%)	1,601 (1.01%)	186 (0.12%)	42 (0.03%)
5–10	181,703 (97.27%)	2,717 (1.45%)	1,857 (0.99%)	377 (0.2%)	102 (0.05%)	43 (0.02%)	178,831 (97.07%)	2,515 (1.37%)	2,243 (1.22%)	533 (0.29%)	85 (0.05%)	31 (0.02%)
10–15	114,039 (99.34%)	377 (0.33%)	278 (0.24%)	62 (0.05%)	28 (0.02%)	13 (0.01%)	113,096 (99.34%)	335 (0.29%)	309 (0.27%)	74 (0.07%)	20 (0.02%)	12 (0.01%)
15–20	56,244 (99.75%)	67 (0.12%)	53 (0.09%)	11 (0.02%)	6 (0.01%)	3 (0.01%)	55,816 (99.79%)	46 (0.08%)	51 (0.09%)	14 (0.03%)	4 (0.01%)	2 (0%)
> 20	36,748 (99.93%)	8 (0.02%)	9 (0.02%)	8 (0.02%)	2 (0.01%)	0 (0%)	36,506 (99.95%)	7 (0.02%)	6 (0.02%)	5 (0.01%)	0 (0%)	0 (0%)

Note: Red pixels in visual maps indicate areas with high concentrations of flooded pixels; blue indicates low concentrations.

PART 5. CRITERIA VALUE RANGES BY SUSCEPTIBILITY CLASS

This table presents the classification thresholds used to categorize each criterion in the flood susceptibility analysis. The classes range from very low (1) to very high (5) susceptibility.

Table S5. Threshold values by flood susceptibility class

Susceptibility class ranges and ratings	**Very low** **1**	**Low** **2**	**Moderate** **3**	**High** **4**	**Very high** **5**
Altitude (m)	1,309–1,644	1,278–1,309	1,261–1,278	1,250–1,261	1,243–1,250
Slope (%)	> 20.87	11.2–20.8	5.2–11.2	0.15–5.25	0–0.15
TWI	2.67–5.43	5.43–6.09	6.09–6.87	6.87–8.39	8.39–11.53
SPI	10.14–76.90	5.46–10.14	2.56–5.46	0.57–2.56	0–0.57
Rainfall (mm/year)	1,064–1,076	1,076–1,098	1,098–1,114	1,114–1,136	1,136–1,177
Landuse	Forestry	Savannah	Agriculture, bare soil	Urban areas	Water bodies
NDVI	0.15–0.54	0.12–0.15	0.10–0.12	0.08–0.10	-0.20–0.08
Distance from river (m)	> 200	150–200	100–150	50–100	0–50
Lithology	Moderate porosity and high permeability	Moderate porosity and permeability	Low to moderate porosity and permeability	Very low porosity and permeability	Very high porosity and low permeability
Flood susceptibility	1.11–2.11	2.11–2.55	2.55–2.99	2.99–3.44	3.44–4.78

PART 6. VALIDATION

1. Validation—Pleiades and Sentinel-1 (Pixels and %)

Table S6. Confusion matrices and accuracy metrics (Pleiades and Sentinel-1)

		Field data (focus groups)		
		F	NF	
Pleiades (2 m × 2 m)	F	112,083 (0.94%)	259,865 (2.19%)	30.13%
	NF	629,381 (5.30%)	10,872,445 (91.38%)	94.53%

		15,12%	97.67%	**92.51%**
Sentinel-1 (10 m × 10 m)	F	96 (0.02%)	954 (0.20%)	9.14%
	NF	29,504 (6.24%)	442,330 (93.54%)	93.75%
		0.32%	99.78%	**93.56%**

F: Flooded; NF: Non-Flooded

2. Validation—FFS (Pixels and %)

Table S7. Confusion matrices and accuracy metrics (FFS)

		Field data (focus groups)		
		F	NF	
FFS-Sim 1 Threshold: 10 cm (30 m × 30 m)	F	2,612 (4.92%)	3,875 (7.30%)	40.27%
	NF	685 (1.29%)	45,916 (86.49%)	98.53%
		79.22%	92.22%	**91.41%**
FFS-Sim 2 Threshold: 10 cm (30 m × 30 m)	F	2,619 (4.93%)	3,797 (7.15%)	40.82%
	NF	678 (1.28%)	45,994 (86.64%)	98.55%
		79.44%	92.37%	**91.57%**
FFS-Sim 3 Threshold: 10 cm (30 m × 30 m)	F	2,549 (4.80%)	3,737 (7.04%)	40.55%
	NF	748 (1.41%)	46,054 (86.75%)	98.40%
		77.31%	92.49%	**91.55%**
FFS-Sim 4 Threshold: 10 cm (30 m × 30 m)	F	2,622 (4.94%)	3,629 (6.84%)	41.95%
	NF	675 (1.27%)	46,162 (86.95%)	98.56%
		79.53%	92.71%	**91.89%**
FFS-Sim 1 Threshold: 25 cm (30 m × 30 m)	F	2,426 (4.57%)	3,627 (6.83%)	40.08%
	NF	871 (1.64%)	46,164 (86.96%)	98.15%

		73.58%	92.72%	**91.53%**
FFS-Sim 2 Threshold: 25 cm (30 m × 30 m)	F	2,427 (4.57%)	3,635 (6.85%)	40.04%
	NF	870 (1.64%)	46,156 (86.94%)	98.15%
		73.61%	92.70%	**91.51%**
FFS-Sim 3 Threshold: 25 cm	F	2,400 (4.52%)	3,577 (6.74%)	40.15%
	NF	897 (1.69%)	46,214 (87.05%)	98.10%
		72.79%	92.82%	**91.57%**
FFS-Sim 4 Threshold: 25 cm (30 m × 30 m)	F	2,464 (4.64%)	3,473 (6.54%)	41.50%
	NF	833 (1.57%)	46,318 (87.25%)	98.23%
		74.73%	93.02%	**91.89%**

F: Flooded; NF: Non-Flooded

3. Validation—MCA (Pixels and %)

Table S8. Confusion matrices and accuracy metrics (MCA)

		Field data (focus groups)		
		F	NF	
MCA (30 m × 30 m)	F	2,247 (4.23%)	2,783 (5.24%)	44.67%
	NF	1,050 (1.98%)	47,008 (88.55%)	97.82%
		68.15%	94.41%	**92.78%**

F: Flooded; NF: Non-Flooded

4. Visual validation maps

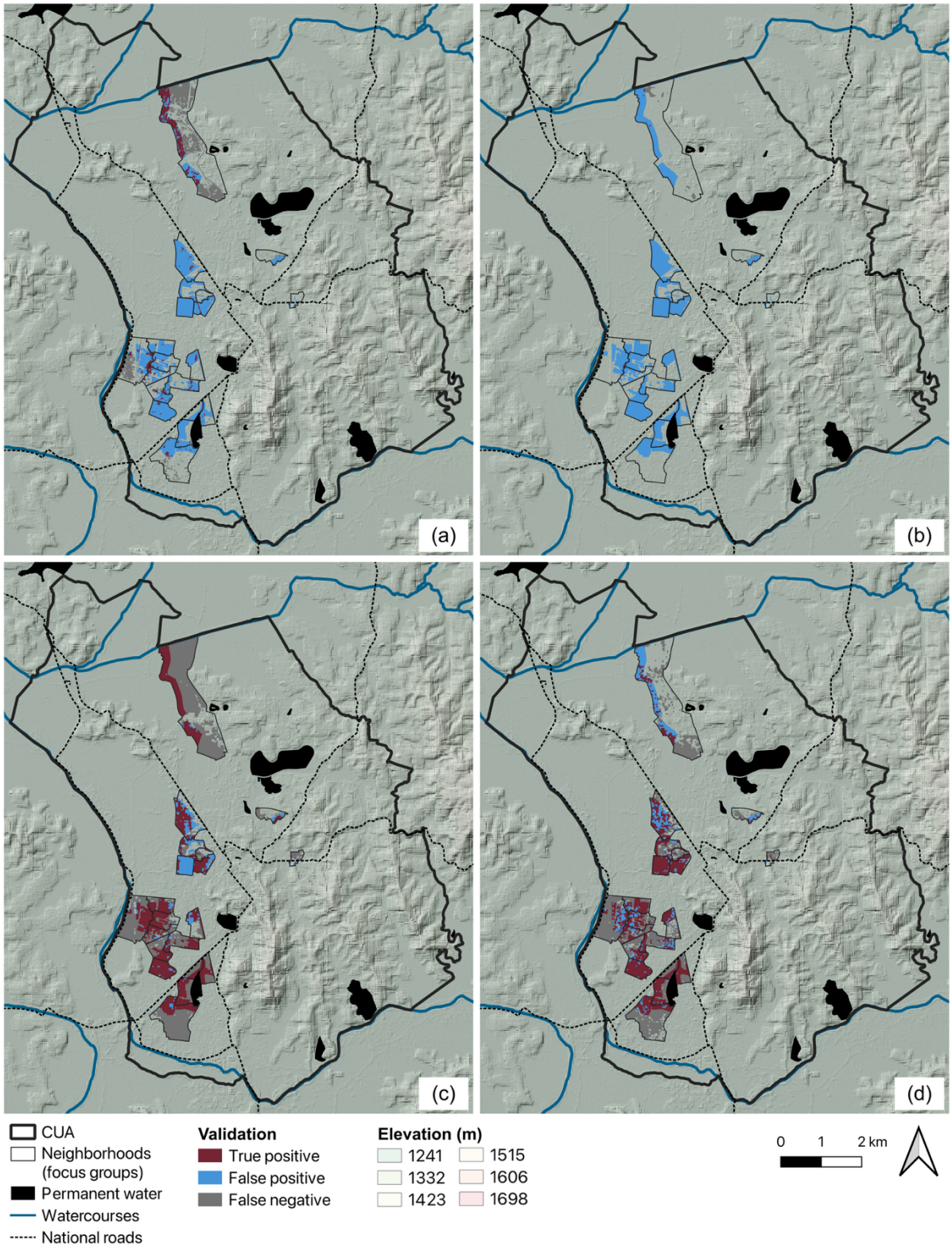

Fig. S4. Validation—CUA scale: a. Field data vs. Pleiades; b. Field data vs. Sentinel-1; c. Field data vs. FFS-Sim 4 (10 cm—corrected DEM); d. Field data vs. MCA

PART 7. IMPACT ASSESSMENT

1. Flooded areas categorized by land use

Table S9. Flooded areas by land use and detection method

	CUA (ha and %)					Peripheral communes (ha and %)			
	Pleiades	**Sentinel-1**	**FFS Sim 4 10 cm**	**FFS Sim 4 25 cm**	**MCA**	**Sentinel-1**	**FFS Sim 4 10 cm**	**FFS Sim 4 25 cm**	**MCA**
Flooded areas	1,448.5 (17.04%)	253.4 (2.98%)	3,845.3 (45.23%)	3,580.1 (42.11%)	3,291.6 (38.72%)	3,890.5 (6.11%)	20,144.7 (31.63%)	18,622.2 (29.24%)	12,143.3 (19.07%)
Forestry	3.6 (0.66%)	0.3 (0.06%)	31.4 (5.79%)	23.8 (4.38%)	6.7 (1.23%)	2.04 (0.07%)	130.7 (4.45%)	97.9 (3.33%)	17.9 (0.61%)
Extractive and construction sites	81,9 (25.65%)	36.7 (11.51%)	222.6 (69.71%)	214.2 (67.07%)	173.6 (54.38%)	247.2 (7.22%)	1,362.7 (39.77%)	1,303.5 (38.04%)	1,027.7 (29.99%)
Wetlands	261.3 (24,67%)	11.4 (1.08%)	750.4 (70.85%)	725 (68.46%)	438.7 (41.42%)	398.5 (18.32%)	1,369.2 (62.93%)	1,327 (60.99%)	987.9 (45.40%)
Savannah and natural vegetation	0,2 (0.13%)	0.002 (0.00%)	16.1 (8.37%)	12.4 (6.43%)	5.8 (2.99%)	28.1 (0.14%)	604.8 (3.08%)	408.5 (2.08%)	122.7 (0.62%)
Bare soil	0.2 (0.43%)	0 (0.00%)	14.1 (33.91%)	9.3 (22.46%)	4.9 (11.85%)	0.50 (0.06%)	120.4 (13.43%)	105.81 (11.80%)	75.43 (8.41%)
Residential areas	25.6 (0.78%)	0.06 (0.00%)	656.1 (19.87%)	548.1 (16.60%)	944.9 (28.62%)	0.11 (0.00%)	502.5 (7.24%)	413.9 (5.96%)	998.6 (14.39%)
Industrial, commercial, and military areas	15.5 (1.88%)	0 (0.00%)	299.8 (36.39%)	239.8 (29.11%)	464.7 (56.41%)	2.01 (0.21%)	178.1 (18.57%)	148.1 (15.45%)	317.2 (33.08%)
Agriculture	1,060.2 (47.76%)	204.9 (9.23%)	1,854.8 (83.55%)	1,807.5 (81.42%)	1,252.3 (56.41%)	3,211.9 (12.03%)	15,876.1 (59.45%)	14,817.3 (55.49%)	8,595.9 (32.19%)

2. Distribution of flooded residential buildings in CUA by land use type

Table S10. Distribution of flooded residential buildings—number and % (*)

	Sentinel-1	Pleiades	FFS Sim 4 10 cm	FFS Sim 4 25 cm	MCA
Forestry	1 (0.00%)	8 (0.00%)	70 (0.03%)	53 (0.02%)	36 (0.01%)
Extractive and construction sites	30 (0.00%)	177 (0.07%)	706 (0.27%)	648 (0.25%)	564 (0.22%)
Wetlands	4 (0.00%)	513 (0.20%)	5,284 (2.02%)	4,981 (1.90%)	3,548 (1.35%)
Savannah and natural vegetation	0 (0.00%)	1 (0.00%)	9 (0.00%)	8 (0.00%)	13 (0.00%)
Bare soil	0 (0.00%)	0 (0.00%)	6 (0.00%)	2 (0.00%)	4 (0.00%)
Residential areas	8 (0.00%)	1,239 (0.47%)	58,663 (22.39%)	50,988 (19.46%)	83,361 (31.81%)
Industrial, commercial, and military areas	0 (0.00%)	189 (0.07%)	5,747 (2.19%)	4777 (1.82%)	8,373 (3.20%)
Agriculture	31 (0.01%)	399 (0.15%)	2,070 (0.79%)	1,863 (0.71%)	1,148 (0.44%)

(*) The percentages have been calculated based on the total number of buildings in the CUA

3. Spatial visualization of impacted buildings

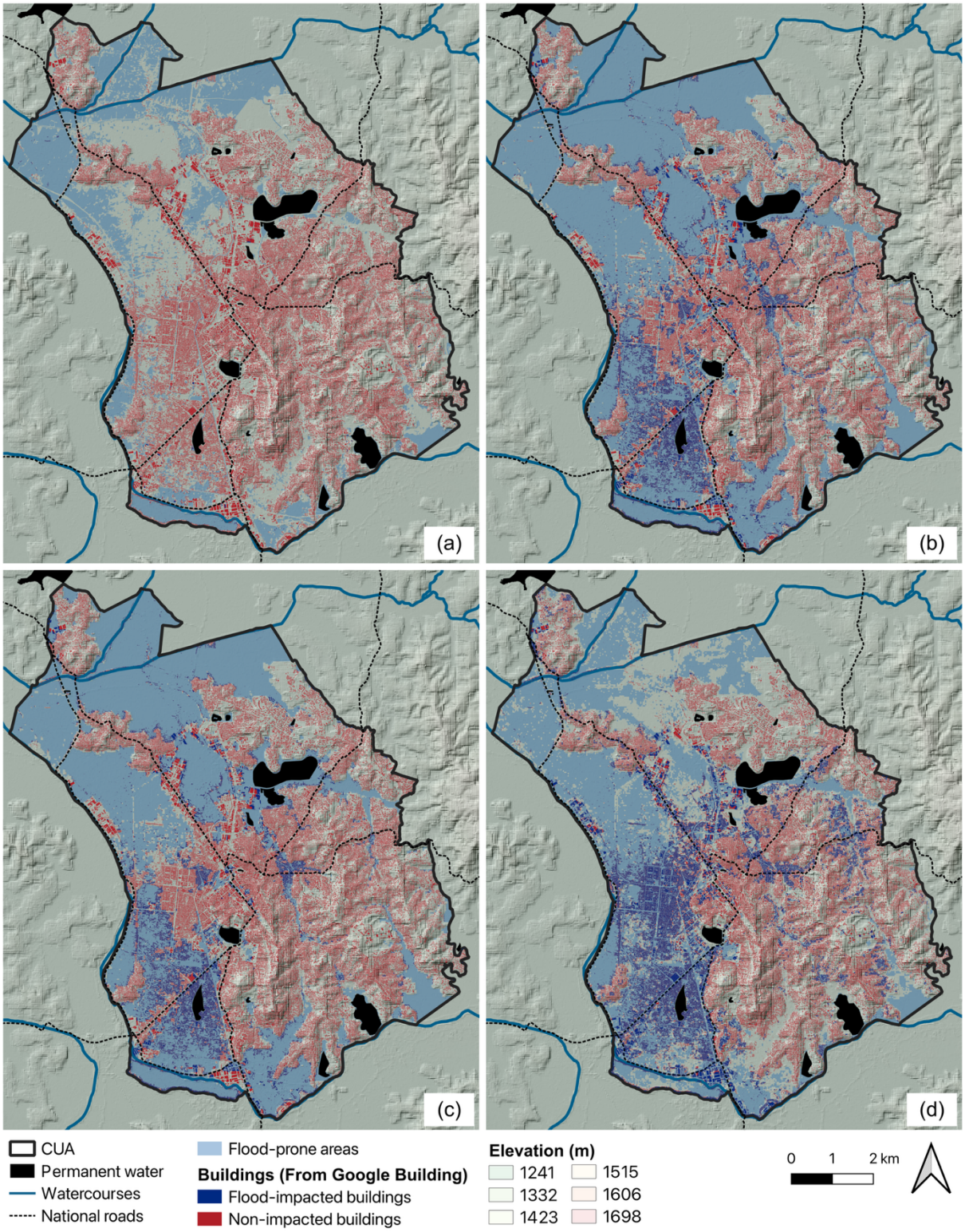

Fig. S5. Spatial distribution of residential buildings impacted and not impacted by flooding: a. Pleiades; b. FFS-Sim 4 (10 cm); c. FFS-Sim 4 (25 cm); d. MCA

References

Andriamamonjisoa SN, Hubert-Ferrari A (2019) Combining geology, geomorphology and geotechnical data for a safer urban extension: application to the Antananarivo capital city (Madagascar). J Afr Earth Sci 151:417–437. https://doi.org/10.1016/j.jafrearsci.2018.12.003

ARTELIA (2020) Mission de maîtrise d'œuvre pour l'extension du schéma directeur d'assainissement d'Antananarivo et modélisation du risque d'inondation au niveau de l'agglomération. Rapport technique. Antananarivo, Madagascar

Beven KJ, Kirkby MJ (1979) A physically based, variable contributing area model of basin hydrology. Hydrol Sci Bull 24:43–69. https://doi.org/10.1080/02626667909491834

Bizzi S, Lerner DN (2015) The use of stream power as an indicator of channel sensitivity to erosion and deposition processes. River Res Applic 31:16–27. https://doi.org/10.1002/rra.2717

Denis A (2019) Adapted transcription of ESA Echoes in Space-Hazard: Flood mapping with Sentinel-1 tutorial (ESA EO College)

Fahrland E, Paschko H, Jacob P, Kahabka H (2022) Copernicus Digital Elevation Model: product handbook. European Space Agency

Hojati M, Mokarram M (2016) Determination of a topographic wetness index using high resolution digital elevation models. Eur J Geogr 7:41–52

Khosravi K, Shahabi H, Pham BT, et al (2019) A comparative assessment of flood susceptibility modeling using multi-criteria decision-making analysis and machine learning methods. J Hydrol 573:311–323. https://doi.org/10.1016/j.jhydrol.2019.03.073

Kopecký M, Čížková Š (2010) Using topographic wetness index in vegetation ecology: does the algorithm matter? Appl Veg Sci 13:450–459. https://doi.org/10.1111/j.1654-109X.2010.01083.x

Laur H, Bally P, Meadows P, et al (2002) Derivation of the backscattering coefficient σ0 in ESA ERS SAR PRI products. In: Proc. of the Second International Workshop on ERS Applications. p 139

McVittie A (2019) Sentinel-1 flood mapping tutorial. Report

Moore ID, Grayson RB, Ladson AR (1991) Digital terrain modelling: A review of hydrological, geomorphological, and biological applications. Hydrol Process 5:3–30. https://doi.org/10.1002/hyp.3360050103

Nibigira L (2019) Etude des risques naturels liés aux interactions entre les mouvements de masse et le réseau hydrographique dans la région des lacs Kivu et Tanganyika.

Université de Liège
Rakotoarimanana ZMH, Rakotovao SR (2022) Analysis of vulnerability and resilience of the population: case of flood in January 2022, in Antananarivo City, Madagascar
Ramdani F (2023) Exploring the Earth with QGIS: a guide to using satellite imagery at its full potential. Springer
Recanatesi F, De Santis A, Gatti L, et al (2025) A comparative analysis of spatial resolution Sentinel-2 and Pleiades imagery for mapping urban tree species. Land 14:106. https://doi.org/10.3390/land14010106
Selmi L (2021) Flood mapping using the Sentinel-1 imagery and the ESA SNAP S1 toolbox. Dati Aperti
Van den Bout B (2024) FastFlood docs. In: FastFlood. https://fastflood.org/site/_site/docs/home/